

Machine learning for data-driven design of AM materials and processes

Gareth Conduit

Machine learning to

Model datasets where the data is **sparse**

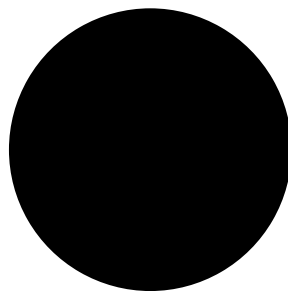
Exploit **property-property** relationships

Merge data, computer simulations, and physical laws

Reduce costly experiments to **accelerate** discovery

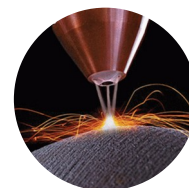
Black box machine learning for materials design

Composition



Properties

Defects



Fatigue



Strength



Train the machine learning

63658497050818
70381840646500
50106637890290
71526909467444
01140449749480
48868527611099
20333272199499
97657934224341
39404670396039
59769286811239
37641343948734

Composition



29392876479090
02136401036020
63658497050818
70381840646500
50106637890290
71526909467444
01140449749480
48868527611099
20333272199499
97657934224341
39404670396039
59769286811239
37641343948734
36652447275378
14421981032661
80555606952664
98344399488109

Properties

Defects

Fatigue

Strength



Machine learning predicts material properties

Composition



Properties

Defects



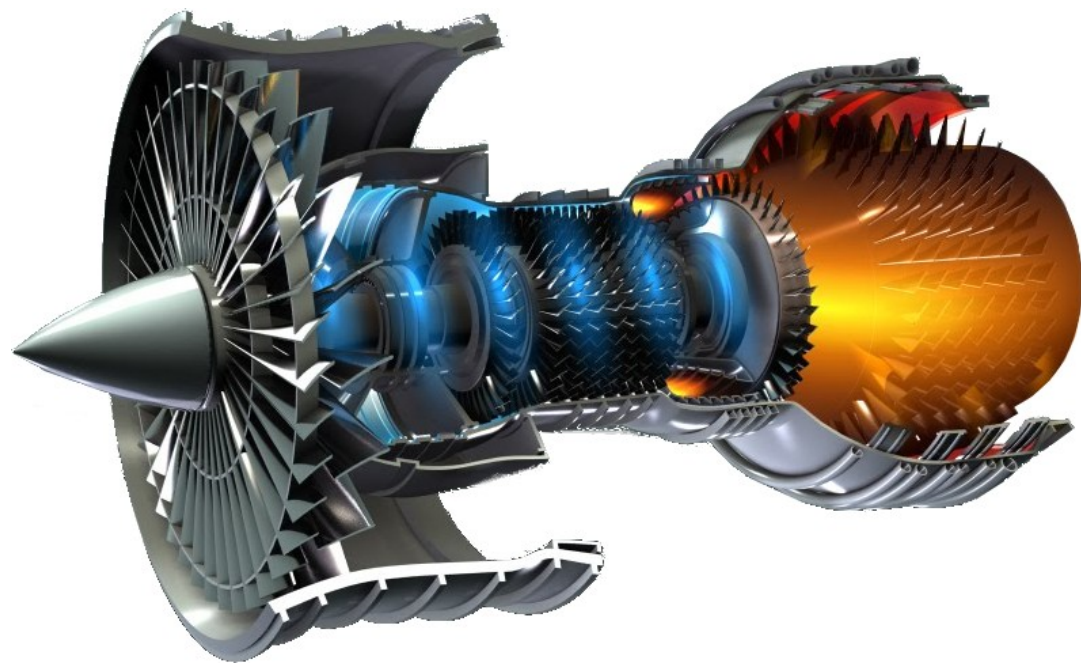
Fatigue



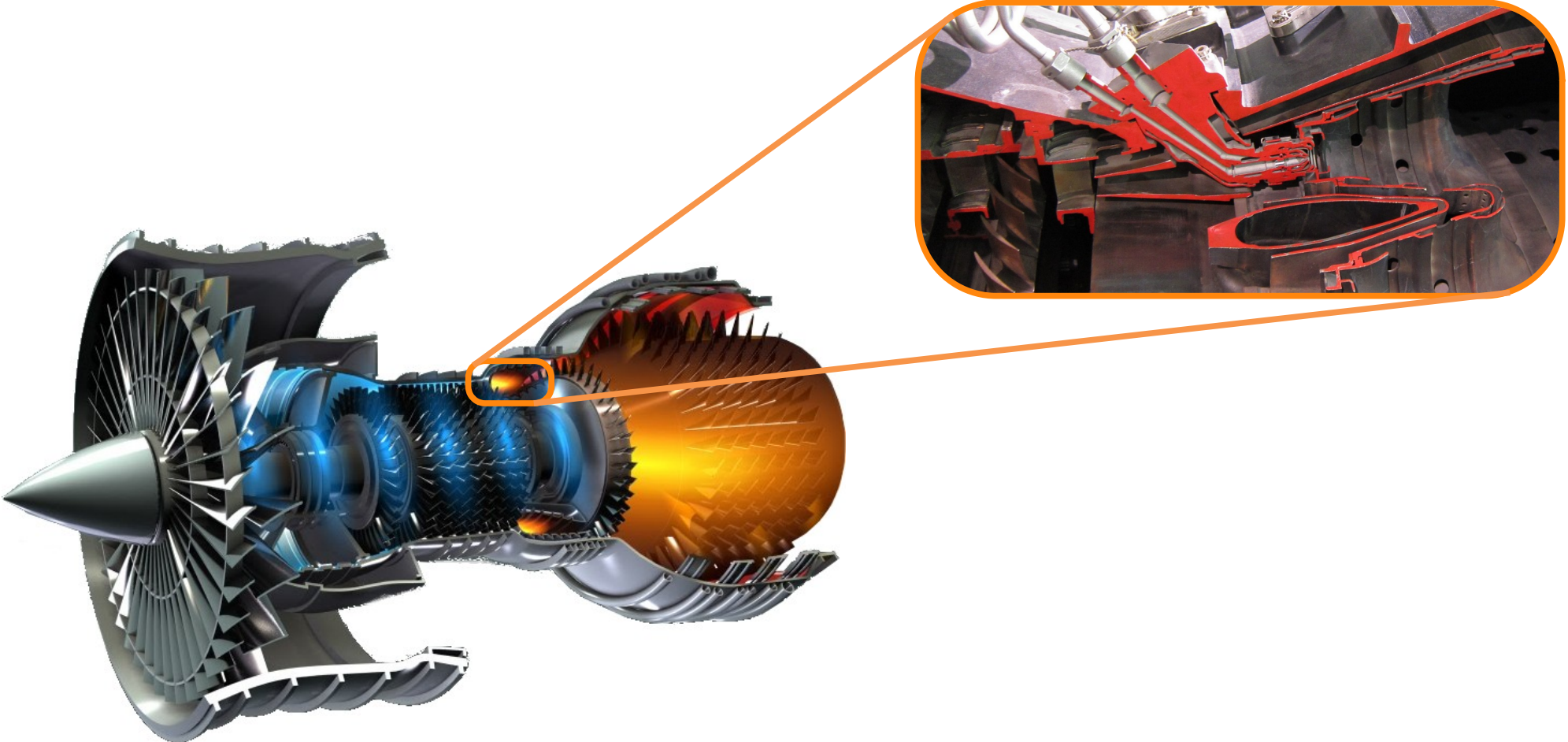
Strength



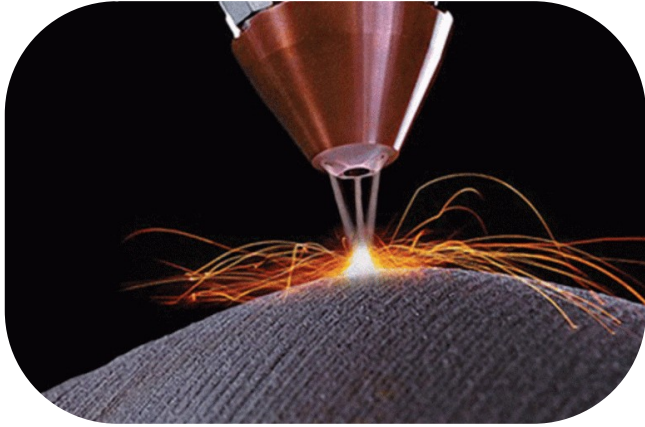
Jet engine schematic



Combustor in a jet engine



Direct laser deposition



Data available to model defect density

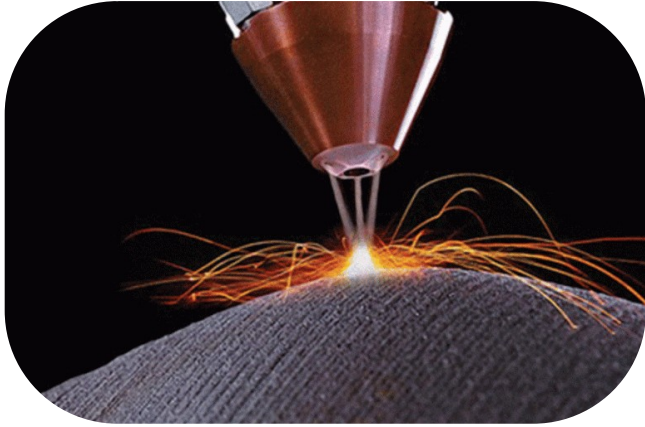


Composition and heat treatment space **30** dimensions

Requires **31** points to fit a hyperplane

Just **10** data entries available to model defect density

Ability for printing and welding are strongly correlated

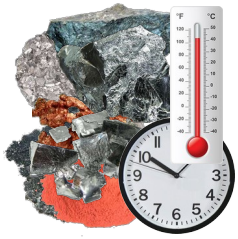


Laser



Electricity

First predict weldability

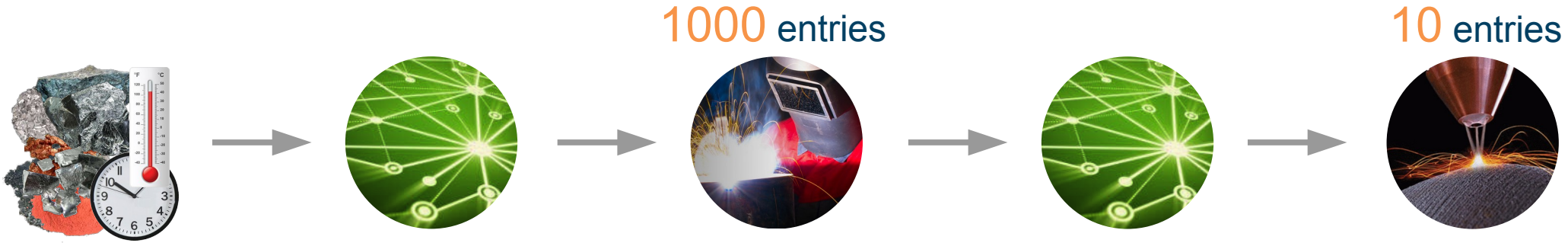


1000 entries



Use 1000 weldability entries to understand complex composition → weldability model

Use weldability to predict defects formed



Use **1000** weldability entries to understand complex composition → weldability model

10 defects entries capture the simple weldability → defect relationship

Two interpolations aid composition → defects **extrapolation**

Use CALPHAD to predict strength



Use **100,000** CALPHAD results to model complex composition → phase behavior

500 strength entries capture the phase behavior → strength relationship

Two interpolations aid the composition → strength **extrapolation**

Target properties

Elemental cost	< 25 \$kg ⁻¹
Density	< 8500 kgm ⁻³
γ' content	< 25 wt%
Oxidation resistance	< 0.3 mgcm ⁻²
Defects	< 0.15% defects
Phase stability	> 99.0 wt%
γ' solvus	> 1000 °C
Thermal resistance	> 0.04 KΩ ⁻¹ m ⁻³
Yield stress at 900 °C	> 200 MPa
Tensile strength at 900 °C	> 300 MPa
Tensile elongation at 700 °C	> 8%
1000hr stress rupture at 800 °C	> 100 MPa
Fatigue life at 500 MPa, 700 °C	> 10 ⁵ cycles

Composition and processing variables

Cr 19%



Co 4%



Mo 4.9%



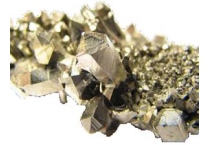
W 1.2%



Zr 0.05%



Nb 3%



Al 2.9%



C 0.04%



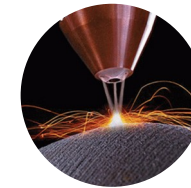
B 0.01%



Ni

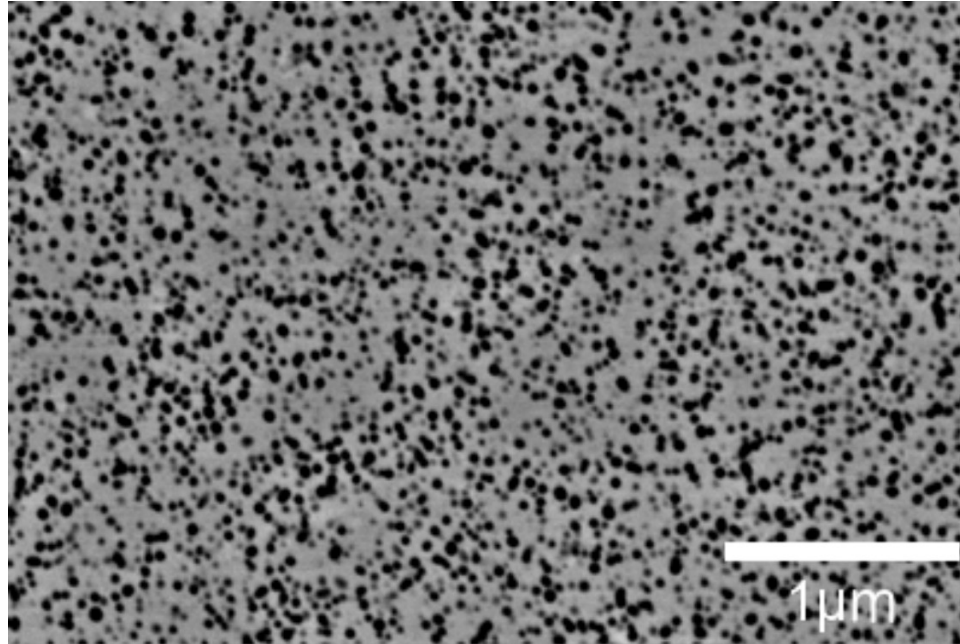


Expose 0.8



T_{HT} 1300°C

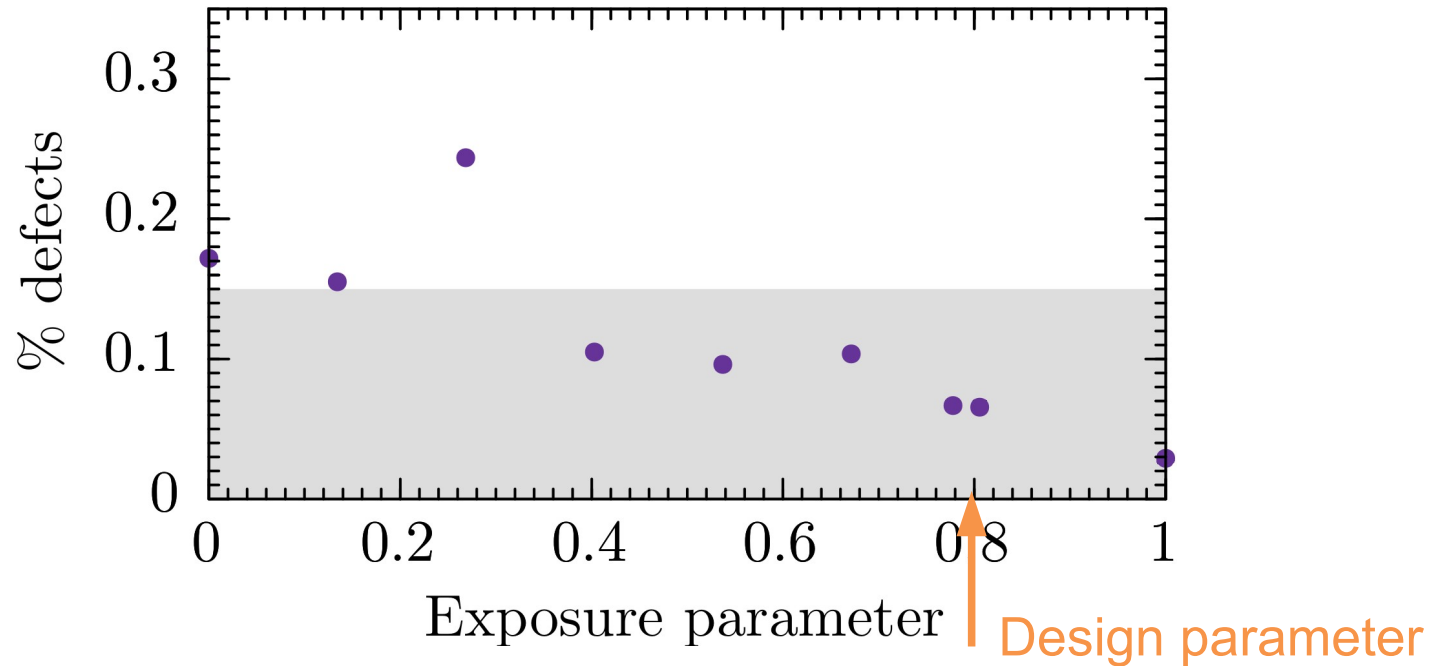




Defects target

Elemental cost	< 25 \$kg ⁻¹
Density	< 8500 kgm ⁻³
γ' content	< 25 wt%
Oxidation resistance	< 0.3 mgcm ⁻²
Defects	< 0.15% defects
Phase stability	> 99.0 wt%
γ' solvus	> 1000 °C
Thermal resistance	> 0.04 KΩ ⁻¹ m ⁻³
Yield stress at 900 °C	> 200 MPa
Tensile strength at 900 °C	> 300 MPa
Tensile elongation at 700 °C	> 8%
1000hr stress rupture at 800 °C	> 100 MPa
Fatigue life at 500 MPa, 700 °C	> 10 ⁵ cycles

Testing the defect density



Probabilistic neural network identification of an alloy for direct laser deposition

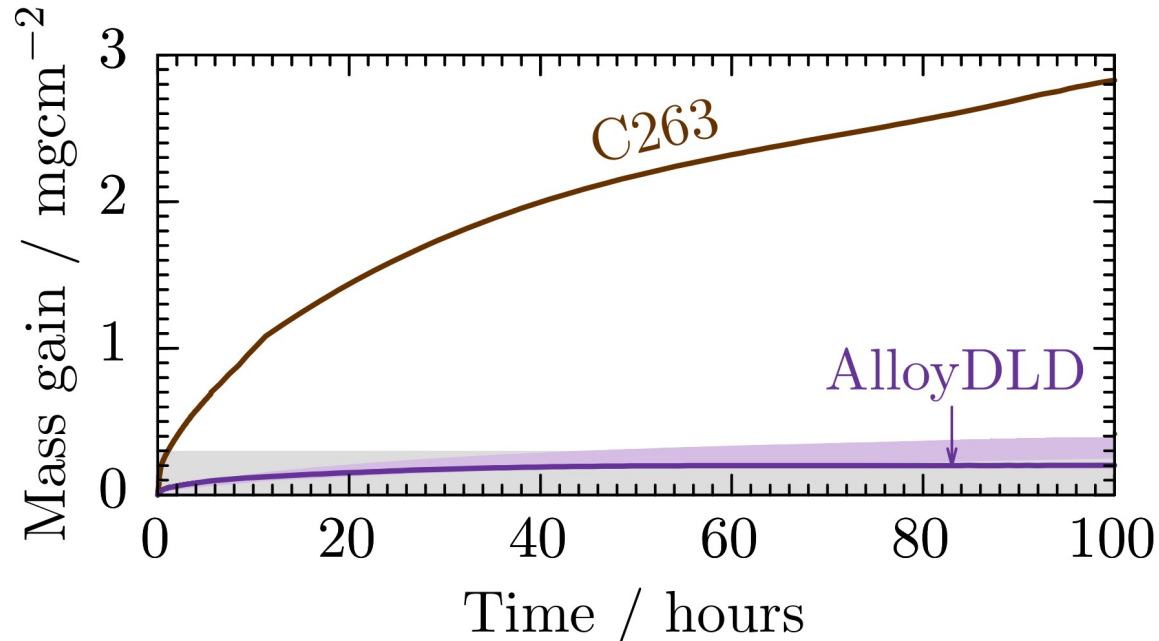
B. Conduit, T. Illston, S. Baker, D. Vadegadde Duggappa, S. Harding, H. Stone & GJC

Materials & Design **168**, 107644 (2019)

Target properties

Elemental cost	< 25 \$kg ⁻¹
Density	< 8500 kgm ⁻³
γ' content	< 25 wt%
Oxidation resistance	< 0.3 mgcm ⁻²
Defects	< 0.15% defects
Phase stability	> 99.0 wt%
γ' solvus	> 1000 °C
Thermal resistance	> 0.04 KΩ ⁻¹ m ⁻³
Yield stress at 900 °C	> 200 MPa
Tensile strength at 900 °C	> 300 MPa
Tensile elongation at 700 °C	> 8%
1000hr stress rupture at 800 °C	> 100 MPa
Fatigue life at 500 MPa, 700 °C	> 10 ⁵ cycles

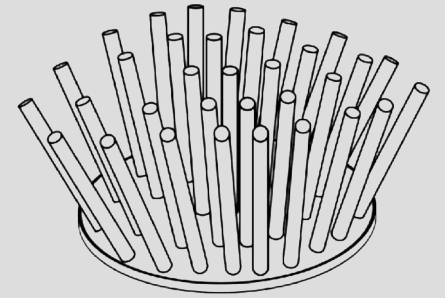
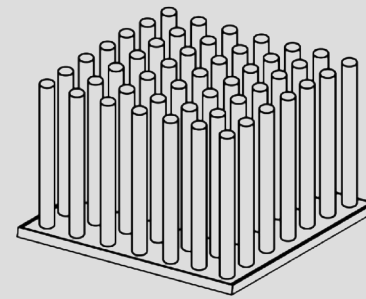
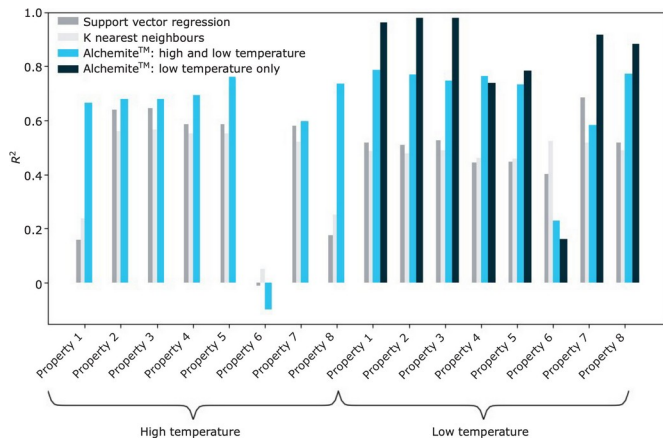
Testing the oxidation resistance



Probabilistic neural network identification of an alloy for direct laser deposition

B. Conduit, T. Illston, S. Baker, D. Vadegadde Duggappa, S. Harding, H. Stone & GJC

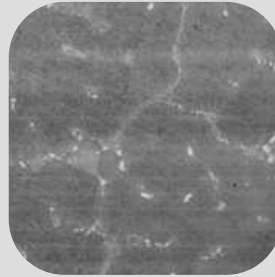
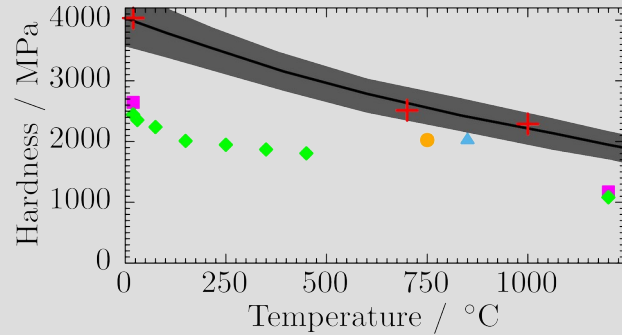
Materials & Design **168**, 107644 (2019)



Johnson Matthey Technology Review
66, 130 (2022)



NASA Technical Memorandum
20220008637



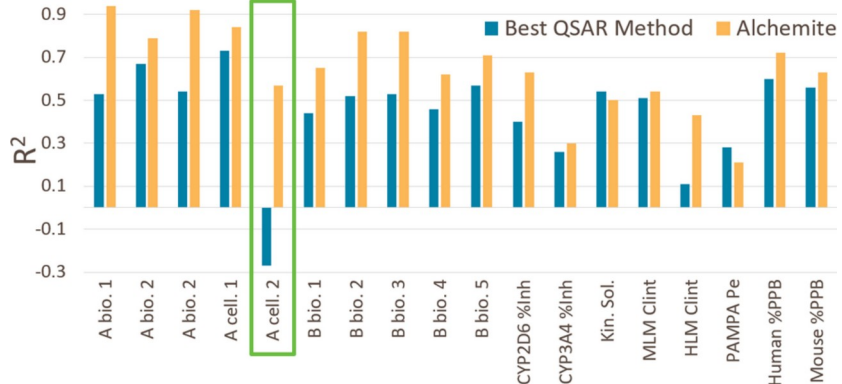
Alloy	Source	ANN	$\Delta\sigma$	Actual
Steel AISI 301L	193	269	5	238[23]
Steel AISI 301	193	267	5	221[23]
Al 1080 H18	51	124	5	120[23]
Al 5083 wrought	117	191	14	300,190[4, 23]
Al 5086 wrought	110	172	11	269,131[4, 23]
Al 5454 wrought	102	149	14	124[23]
Al 5456 wrought	130	201	11	165[23]
INCONEL600	223	278	10	≥ 550 [23]

Materials & Design **131**, 358 (2017)
Scripta Materialia **146**, 82 (2018)
Data Centric Engineering **3**, e30 (2022)



Computational Materials
Science **147**, 176 (2018)





optibrium™

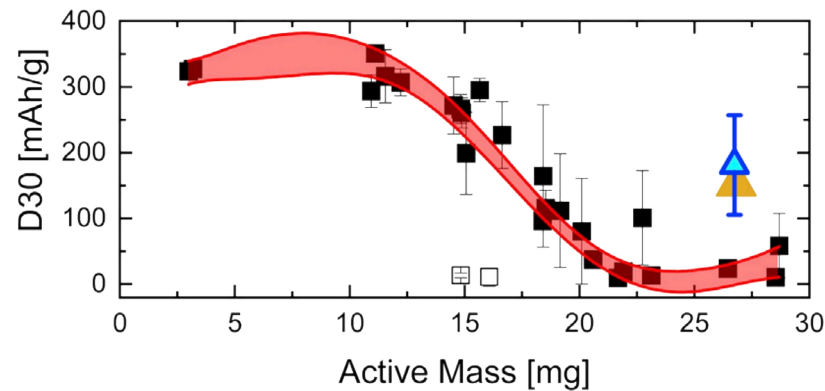
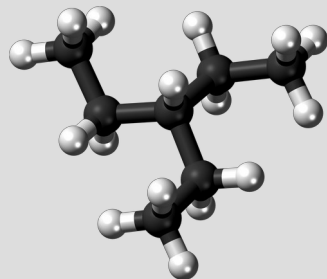
iff



J. of Chem. Info. & Model. **60**, 2848 (2020)
 Applied AI Letters **2**, e31 (2021)
 Molecular Pharmaceutics **19**, 1488 (2022)



Journal of Computer-Aided
 Molecular Design **35**, 112501140 (2021)



Fluid Phase Equilibria **501**, 112259 (2019)
 Journal of Chemical Physics **153**, 014102 (2020)



Cell Reports
 Physical Science
2, 100683 (2021)



UNIVERSITY OF
 BIRMINGHAM



Summary

Merge computer simulations with experimental data and exploit **property-property** relationships to circumvent **missing data**

Designed and **experimentally verified** alloy for direct laser deposition

Generic approach applied to alloys, batteries, pharmaceuticals, and beyond

Taken to market through startup **Intellegens**